ARTICLE
Journal of Cellular Biochemistry 116:2304–2312 (2015)

Journal of Cellular Biochemistry

Resveratrol Regulates the Quiescence-Like Induction of Activated Stellate Cells by Modulating the PPARγ/SIRT1 Ratio

Izabel Cristina Custódio de Souza,[1,2] Leo Anderson Meira Martins,[2*] Mariana de Vasconcelos,[2] Cleverson Moraes de Oliveira,[2] Florencia Barbé-Tuana,[2] Cláudia Balbinotti Andrade,[3] Letícia Ferreira Pettenuzzo,[2] Radovan Borojevic,[4] Rogério Margis,[5] Regina Guaragna,[2] and Fátima Costa Rodrigues Guma[2]

[1]*Departamento de Morfologia, IB, Universidade Federal de Pelotas (UFPel), av. Duque de Caxias, 250 CEP 96 030 000, Pelotas, RS, Brazil*

[2]*Departamento de Bioquímica, ICBS, Universidade Federal do Rio Grande do Sul (UFRGS), rua Ramiro Barcelos, 2600-Anexo I CEP 90035-003, Porto Alegre, RS, Brazil*

[3]*Departamento de Química, ICET, Universidade Federal do Mato Grosso (UFMT), Cuiabá, MT, Brazil*

[4]*Departamento de Histologia e Embriologia, ICB, PABCAM, Universidade Federal do Rio de Janeiro (UFRJ), Rio de Janeiro, RJ, Brazil*

[5]*Departamento de Biofísica, Universidade Federal do Rio Grande do Sul, Porto Alegre, Rio Grande do Sul, Brazil*

ABSTRACT

The activation of hepatic stellate cell (HSC), from a quiescent cell featuring cytoplasmic lipid droplets to a proliferative myofibroblast, plays an important role in liver fibrosis development. The GRX line is an activated HSC model that can be induced by *all-trans*-retinol to accumulate lipid droplets. Resveratrol is known for activating Sirtuin1 (SIRT1), a NAD^+-dependent deacetylase that suppresses the activity of peroxisome proliferator-activated receptor gamma (PPARγ), an important adipogenic transcription factor involved in the quiescence maintenance of HSC. We evaluated the effects of 0.1 μM of resveratrol in retinol-induced GRX quiescence by investigating the interference of SIRT1 and PPARγ on cell lipogenesis. GRX lipid accumulation was evaluated through Oil-red *O* staining, triacylglycerides quantification, and [^{14}C] acetate incorporation into lipids. mRNA expression and protein content of SIRT1 and PPARγ were measured by RT-PCR and immunoblotting, respectively. Resveratrol-mediated SIRT1 stimuli did not induce lipogenesis and reduced the retinol-mediated fat-storing capacity in GRX. In order to support our results, we established a cell culture model of transgenic super expression of PPARγ in GRX cells (GRXPγ). Resveratrol reduced lipid droplets accumulation in GRXPγ cells. These results suggest that the PPARγ/SIRT1 ratio plays an important role in the fate of HSC. Thus, whenever the PPARγ activity is greater than SIRT1 activity the lipogenesis is enabled. J. Cell. Biochem. 116: 2304–2312, 2015.

KEY WORDS: GRX; HEPATIC STELLATE CELLS; LIPID ACCUMULATION; PPARγ; RESVERATROL; SIRT1

Liver fibrosis results from chronic hepatic damage and involves the abnormal accumulation of the extracellular matrix proteins. Advanced stage of liver fibrosis distorts the hepatic architecture by forming fibrous scars. This situation may lead to

Abbreviations: HSC, Hepatic Stellate Cell; PPAR, Peroxisome Proliferator-Activated Receptor; RSV, Resveratro; RHO, Retinol; SIRT1, Sirtuin 1; TG, Triglicerides.

Grant sponsor: Conselho Nacional de Desenvolvimento Científico e Tecnológico (CNPq); Grant sponsor: Coordenação de Aperfeiçoamento de Pessoal de Nível Superior (CAPES); Grant sponsor: Fundação de Amparo à Pesquisa do Estado do Rio Grande do Sul (FAPERGS); Grant sponsor: Pró-Reitoria de Pesquisa da Universidade Federal do Rio Grande do Sul (PROPESQ-UFRGS).

*Correspondence to: Leo Anderson Meira Martins, Ph.D., Departamento de Bioquímica, ICBS, UFRGS, Rua Ramiro Barcelos 2600-anexo, CEP: 90035-003, Porto Alegre, RS, Brazil. E-mail: leo.meira@ufrgs.br

Manuscript Received: 7 January 2015; Manuscript Accepted: 31 March 2015

Accepted manuscript online in Wiley Online Library (wileyonlinelibrary.com): 2 April 2015

DOI 10.1002/jcb.25181 • © 2015 Wiley Periodicals, Inc.

cirrhosis, portal hypertension, and hepatic failure [Bataller and Brenner, 2005].

The hepatic stellate cells (HSC) activation, from a quiescent cell featuring vitamin A stored on lipid droplets to a proliferative myofibroblast, remains among the most informative discoveries on understanding the mechanistic basis of liver fibrosis progression and regression [Friedman, 2008]. HSC activation is a highly pleiotropic process by which phenotypic changes require the global reprogramming of cell gene expression that must be orchestrated by long-term changes in the expression and/or activity of key transcription factors [Cheng et al., 2007]. Strategies for reducing liver fibrosis include the induction of activated HSC apoptosis and the reversion of activated HSC to the quiescent vitamin A-storing phenotype [Friedman, 2008]. The GRX cell line was established from an hepatic fibre granuloma induced by *Schistosoma mansoni* infection in C3H/HeN mice. These cells are a useful tool for liver fibrosis study and represent a HSC model that expresses the activated myofibroblast phenotype. The GRX cells can be in vitro induced to express the quiescent-like lipocyte phenotype by treatment with retinol, β-carotene, indomethacin or capsaicin, resulting in an overall increase of lipid storage [Borojevic et al., 1985; Margis and Borojevic, 1989; Borojevic et al., 1990; Martucci et al., 2004; Guimaraes et al., 2007; Teodoro et al., 2009; Bitencourt et al., 2012].

Peroxisome proliferator-activated receptors (PPAR) are a group of nuclear receptor proteins that act as transcription factors. The PPAR superfamily are composed of PPARα, PPARδ/β, and PPARγ; three subgroups that mainly regulate the expression of several genes involved in lipid metabolism [Desvergne, 2008]. PPARγ is primarily expressed in adipose tissue and is responsible for promoting fat storage by increasing the transcription of a number of lipogenic proteins and by inducing the adipocyte differentiation [Song et al., 1994; Teboul et al., 1995]. Interestingly, it was already shown that PPARγ expression is markedly decreased in activated HSC. On the other hand, culture-activated HSC can be phenotypically and functionally reversed to a quiescent-like phenotype by forced expression of PPARγ [Hazra et al., 2004]. On this premise, it was already demonstrated that PPARγ mRNA expression was increased in GRX quiescent-like cells [Guimaraes et al., 2007; Bitencourt et al., 2012].

The directly or indirectly activation of sirtuin 1 (SIRT1), a highly conserved NAD^+-dependent protein deacetylase, has been pointed for being responsible for several beneficial effects of polyphenols in therapeutic interventions in a variety of chronic diseases. Resveratrol (RSV; 3,5,4′-trihydroxystilbene) is a naturally-occurring phytoalexin that exerts pleiotropic functions through SIRT1 activation. Both RSV and SIRT1 were already suggested to inhibit adipogenesis, a situation that may interfere on the HSC quiescence maintenance [Backesjo et al., 2009; Ahn et al., 2013]. Here we demonstrated the impact of the RSV-induced expression of SIRT1 in the lipogenesis of HSC using the GRX line as a cell culture model. We strengthen our results by the forced expression of PPARγ in GRX cells (GRXPγ). In conclusion, we hypothesized that the PPARγ/SIRT1 mRNA and protein ratio could play an important role in the HSC lipogenesis or activation.

MATERIALS AND METHODS

REAGENTS

All-trans-retinol (RHO), resveratrol (RSV), lipid standards, Oil Red *O*, and the Dulbecco′s Modified Eagle′s Medium (DMEM) were purchased from Sigma Chemical Company (St. Louis, MO). AdipoRed™ was purchased from Lonza (Basel, Switzerland). TRIzol reagent, M-MLV reverse transcriptase, PureLink Quick Gel and Plasmid Miniprep Extraction kit, pcDNA3.1/V5-His TOPO®TA plasmid, Lipofectamine, Geneticin (G418), SuperScript-II RT preamplification system, and Platinum Taq DNA polymerase were purchased from Invitrogen Inc. (Carlsbad, CA). Plates and all solvents for thin layer chromatography (TLC) were purchased from Merck (Darmstadt, Germany). Fetal bovine serum (FBS) was purchased from Cultilab (Campinas, Brazil).

CELL CULTURE

The murine HSC cell line, GRX, was established by Borojevic and kindly provided by the Cell Bank of Rio de Janeiro (HUCFF, UFRJ, RJ, Brazil). Cells were routinely maintained in DMEM supplemented with 5% FBS and 2 mg/ml HEPES buffer, pH 7.4, at 37°C and 5% CO_2.

PREPARATION OF STABLE GRXPγ CELL LINE

To establish the GRXPγ cell line that super expresses PPARγ, cDNA for PPARγ was amplified from GRX cell line using the specific primer sequences for the full gene (forward: 5′-TAT GGG TGA AAC TCT GGG AG-3′; reverse: 5′-CTA ATA CAA GTC CTT GTA GAT C-3′) cloned into pcDNA 3.1/V5-His TOPO®TA expression vector. The recombinant plasmid pcDNA-PPARγ was amplified through by thermal shock transformation of *Escherichia coli* JM109 competent cells, and purified using the PureLink Quick Plasmid Miniprep kit. PPARγ cDNA sequence was confirmed by sequencing in ABI-PRISM 3100 Genetic Analyzer (Applied-Biosystem, NY). The pcDNA-PPARγ was transfected in GRX cells at 50–60% of confluence with Lipofectamine and 0.3 μg of pcDNA-PPARγ. After 72 h, transfected cells were selected by 1000 μg/mL of Gentamicin 418 (G418) for 4 weeks. During experimental series, G418 concentration was reduced to 500 μg/mL.

CELL TREATMENT

GRX and GRXPγ were plated in 12-well plates (5×10^4 cells/ml) and cultured for 24 h to reach 60–70% confluence before treatments. RHO stock solution has been prepared as previously described [Margis and Borojevic, 1989; Guimaraes et al., 2007]. The final concentration of RHO (5 μM) and RSV (0.1 μM) in the culture medium was obtained by serial dilution. The GRX fat-storing phenotype was induced by treating cells with RHO [Margis and Borojevic, 1989]. The GRX cells were treated with RSV, RHO, or RHO and RSV for 120 h. For RT-PCR experiments, GRX cells were also treated for 12 and 24 h. The GRXPγ cell line was treated with RSV for 120 h. Thus, we intended to understand the effects of RSV in the PPARγ expression. Vehicle treated cells were used as controls.

QUANTIFICATION OF TRIACYLGLYCERIDES CONTENT AND LIPID ACCUMULATION ANALYSIS

Intracellular lipid droplets in GRX cells were identified by standard Oil-Red-O staining. Cells were visualized at x100 magnification under bright field of an inverted microscope (Nikon Eclipse TE 300, Japan).

Untreated and treated GRX cells were assayed for triacylglyceride (TG) content using Triglycerides Liquiform kit (Labtest, MG, Brazil). To compare lipid accumulation between GRX and GRXPγ, cells were stained with AdipoRed™ reagent in PBS for 15 min and loaded into a plate fluorimeter reader (M5, Molecular Devices, CA), after exciting at 490 nm, and collecting the emission at 570–590 nm. Results were normalized to correspondent protein content, measured according to Peterson [Peterson, 1979].

LIPID SYNTHESIS

Lipid synthesis was monitored by acetate incorporation. Untreated and GRX treated cells were incubated for the last 16 h of culture with 0.1 μCi/ml [2-^{14}C] acetic acid sodium salt (56.0 mCi/mmol, Amershan Life Science, UK). After incubation, lipids were extracted using the Folch method [Folch et al., 1957]. The chloroform phase was dried under nitrogen and the radioactive lipid separated by TLC in hexane:ethyl ether:acetic acid (90:10:1; v/v/v). The radioactive lipids were visualized by autoradiography of TLC plates, identified by comparison with standards, and quantified by densitometry of the radiographic film. Results were normalized to the correspondent protein sediments measured according to Peterson [1979].

IMMUNOBLOTTING

Cell samples were lysed in Tris–HCl buffer (pH 6.8) with 2% SDS, 10% glycerol, and 2- β-mercaptoethanol. Equal amounts of protein were loaded onto 10% SDS–PAGE, transferred to nitrocellulose membranes (Hybond ECL Nitrocellulose Membrane, Amersham), and immunoblotted with the appropriate antibodies. Primary antibodies PPARγ (E-8) and SIRT1 (H-300) were purchased from Santa Cruz (CA); β-actin (#4967) from Cell Signaling Technologies (MA). HRP-conjugated anti-rabbit or anti-mouse-IgG antibodies were also purchased from Santa Cruz. Proteins were detected by chemiluminescence (ECL detection system, Amersham Pharmacia, UK). Bands intensities were quantified by densitometry using Alpha Ease FC software (version 6.0.0, Genetic Technology Inc., Miami, FL).

REAL-TIME PCR

Total RNA was isolated using TRIzol Reagent. 2 μg of total RNA was added to each cDNA synthesis reaction, using the SuperScript-II RT pre-amplification system. Reactions were performed at 42°C for 1 h using the T23V primer (5′ TTT TTT TTT TTT TTT TTT TTT TTV). PCR amplification was carried out using specific primer pairs designed by Oligo Calculator version 3.02 (http://basic.nwu.edu/biotools/oligocalc.html) and synthesized by RW-Genes (RJ, Brazil). Primer sequences are listed in Table I. RNA expression levels were quantified using SYBR Green on StepOnePlus real-time cycler (Applied-Biosystems, Grand Island, NY) and performed in quadruplicate in a final volume of 20 μlc. Reactions were composed of 10 μL of each reverse transcription sample diluted 50 to 100 times, 2 μL of 10× PCR buffer, 1.2 μL of 50 mM $MgCl_2$, 0.4 μL of 5 mM dNTPs, 0.4 μL of 10 μM primer pairs, 3.95 μL of H_2O milli-Q, 2.0 μL of SYBR green (1:10,000, Molecular Probe), and 0.05 μL of Platinum Taq DNA polymerase (5 U/μL) (Invitrogen). Reaction settings included an initial denaturation step of 5 min at 94°C followed by 40 cycles of 10 s at 94°C, 15 s at 60°C, 15 s at 72°C, and 35 s at 60°C for data acquisition; samples were kept for 2 min at 40°C for annealing and then heated from 55 to 99°C at a rate of 0.1°C/s to produce the denaturing curve of the amplified products. All results were analyzed by the $2^{-\Delta\Delta CT}$ method [Livak and Schmittgen, 2001]. β-actin was used as the internal control gene for all relative expression calculations [Guimaraes et al., 2006].

TABLE I. Primer sequences

Gene	Primer sequences	GenBank reference
PPARγ	Forward - 5′ TGG AAT TAG ATG ACA GTG ACT TGG 3′ Reverse - 5′ CTC TGT GAC GAT CTG CCT GAG 3′	NM_011146.3
SIRT 1	Forward - 5′ GGC TTG AGG GTA ATC AAT ACC TG 3′ Reverse - 5′ AAA CTT GGA CTC TGG CAT GTG 3′	NM_001159589.1
β-Actin	Forward - 5′ TAT GCC AAC ACA GTG CTG TCT GG 3′ Reverse - 5′ TAC TCC TGC TTG CTG ATC CAC AT 3′	NM_007393.3

STATISTICAL ANALYSIS

Results are from three independent experiments (n = 3). Data were expressed as mean ± standard deviation of the mean. One-way ANOVA was used. When indicated, a post hoc Duncan multiple range test was performed. Values were considered statistically different when P values were equal to or less than 0.05.

RESULTS

GRX TREATED WITH RSV AND RHO ACCUMULATES LIPID DROPLETS DESPITE THE LOWER LIPOGENESIS

To define the role of RSV on lipid accumulation in HSC, GRX were treated with 0.1 μM of RSV, 0.5 μM of RHO, or co-treated with RHO and RSV for 120 hours. Optical microscopy analysis of Oil-red O stained cells revealed that untreated and RSV-treated GRX presented similar characteristics and did not accumulated lipid droplets. In contrast, RHO and co-treated cells had an increase in lipid droplets accumulation, an important feature of the quiescent HSC phenotype (Fig. 1A). The determination of cellular TG content confirmed the morphological analysis (Fig. 1B). The 'de novo' synthesis of TG in RSV-treated group was similar to GRX control cells. Interestingly, only RHO-treated cells exhibited an increase of [^{14}C] acetate incorporation into TG (Fig. 1C).

PPARγ/SIRT1 BALANCE IS CRUCIAL FOR GRX LIPOGENESIS

RSV is well known for inducing SIRT1 activity. Because of the important role of SIRT1 and PPARγ on fat metabolism, we quantified these proteins by immunoblotting. After 120 h of treatment, protein expression revealed a tendency towards an up-regulation of PPARγ in RHO- and co-treated cells, whereas RSV-treated cells presented an

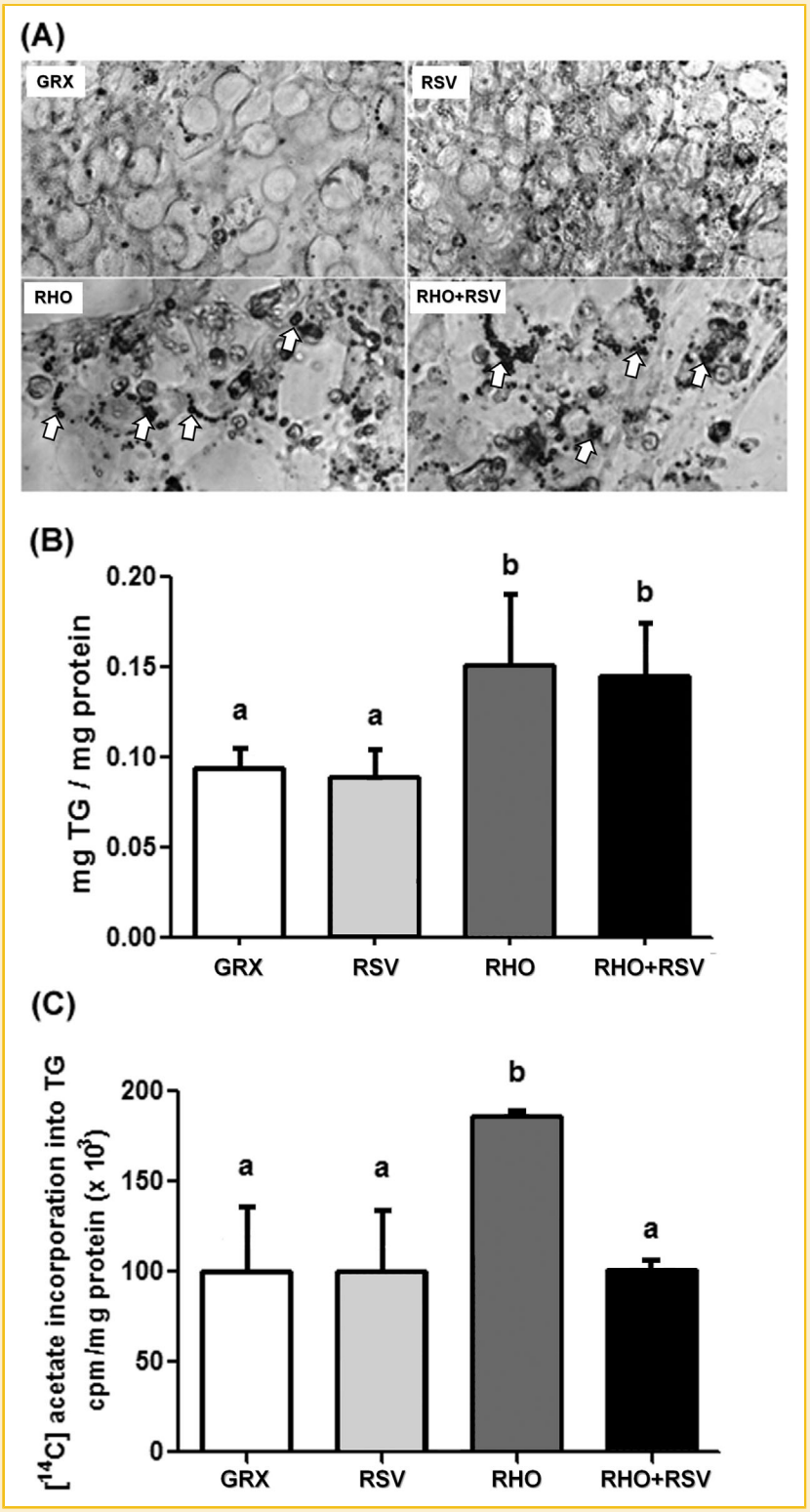

Fig. 1. GRX lipogenesis. Phase contrast images of GRX cells stained with Oil Red-O. White arrows point the lipid droplets accumulation in the RHO-treated and co-treated cells (A). RHO-and co-treated cells presented an increase in the intracellular TG, corroborating imaging analysis (B). Only RHO-treated cells presented an increase in the lipogenesis although co-treated cells have also presented intracellular lipid droplets. Results were expressed as percentage of total radioactivity incorporated (C). Means without a common letter are statistically different ($n = 3$, $P \leq 0.05$).

increase of SIRT1 content (Fig. 2A). In this regard, when we evaluated the PPARγ/SIRT1 balance at the protein level, we found that PPARγ content was favored in RHO and co-treated cells (Fig. 2B).

To further clarify our results, we evaluated the mRNA expression for PPARγ and SIRT1 after 12, 24, and 120 h of treatment. To our surprise, SIRT1 mRNA expression was increased in all experimental groups in a time-dependent manner when comparing to the 12-hour cultured GRX group. Furthermore, it was noticeable that the RHO-induced increase of PPARγ mRNA expression occurred faster than the RSV-induced increase of SIRT1 mRNA expression (Fig. 2C). Indeed, after 12 h of treatment, RHO-treated cells presented an increase in the PPARγ mRNA expression, while no differences in the SIRT1 mRNA expression were observed among the groups. After 24 h, RHO-treated cells presented an increase in PPARγ expression (mRNA level) that was significantly higher in co-treated cells. At this point, only co-treated cells presented a slight significant increase in the SIRT1 mRNA expression. After 120 h, treatment with RSV triggered a significant increase of SIRT1 mRNA expression and did not change the PPARγ mRNA expression. Contrary, treatment with RHO did not change the mRNA expression of SIRT1; but triggered an increase on the PPARγ mRNA expression in GRX. Interestingly, co-treatment with RHO and RSV promoted an increase of PPARγ mRNA expression that was significantly higher than control cells, but lower than RHO-treated cells. Co-treatment triggered a decrease of SIRT1 mRNA content when compared to other groups (Fig. 2C). Considering possible effects of SIRT1 on PPARγ, we established a ratio between their mRNA expression. Cells treated with RSV presented a PPARγ/SIRT1 ratio (at mRNA level) similar to that found in untreated cells at 12, 24, and 120 h of treatment. On the other hand, PPARγ mRNA expression was favored over the SIRT1 mRNA expression in cells treated with RHO for 12, 24, and 120 h. In co-treated cells, the PPARγ/SIRT1 ratio increased similarly to RHO-treated cells after 24 h of treatment. Interestingly, after 120 h, co-treated cells presented higher values comparing to untreated or RSV-treated groups that were lower to that found for RHO-treated group (Fig. 2D).

RESVERATROL TREATMENT REDUCES LIPID DROPLETS ACCUMULATION IN GRXPγ CELLS

With the intention of comparing lipid accumulation and because of the central role of PPARγ in lipogenesis of HSC, we established a cell

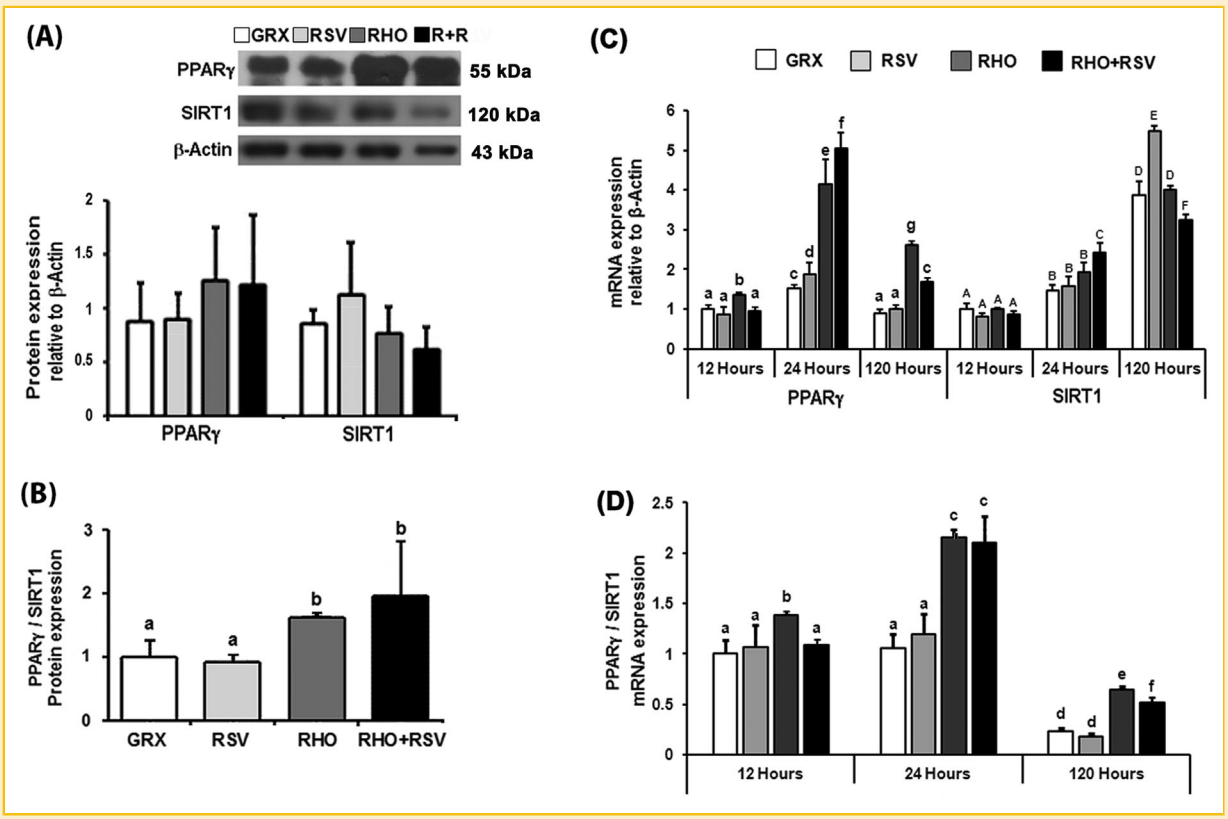

Fig. 2. Measurement of the PPARγ and SIRT1 protein content and analysis of their mRNA expression. The protein content of SIRT1 and PPARγ was measured after 120 h of treatment and was not statistically significant (A). However, when it was established the PPARγ/SIRT1 ratio for the protein content, it was found a significant increase of PPARγ over SIRT1 (B). RT-PCR was performed to evaluate the mRNA expression of PPARγ and SIRT1 after 12, 24, and 120 h of GRX treatment. Results were related to mRNA expression of untreated GRX cultured for 12 h. Under all experimental conditions, the expression of SIRT1 mRNA gradually increased with culture time. RHO increased PPARγ expression after 24 h of treatment whereas RSV increased SIRT1 expression after 120 h of treatment (C). The PPARγ/SIRT1 ratio for mRNA expression was significantly higher in co-treated cells than RHO-treated cells after 24 h of treatment, whereas the opposite was observed after 120 h of treatment (D). Means without a common letter are statistically different ($n = 3$, $P \leq 0.05$).

line designed GRXPγ, that super expresses PPARγ. Immunoblot analysis confirmed an up-regulation of approximately 30% increase in PPARγ protein content in GRXPγ cells (Fig. 3A). Curiously, the PPARγ overexpression by itself promotes a 4-fold increase in GRXPγ lipid accumulation when compared to GRX, and RSV decreased this GRXPγ capacity by almost half (Fig. 3B). As expected, the PPARγ mRNA was 8-fold increased in transfected cells, but RSV treatment was not able to reduce this expression pattern. On the other hand, GRXPγ cells presented a slight reduction in SIRT1 mRNA expression (Fig. 3C). Finally, the ratio between the PPARγ and SIRT1 mRNA expression revealed that the adipogenic transcription factor was favored in GRXPγ cells. RSV treatment induced a reduction in the PPARγ/SIRT1 ratio that remained higher than that found in GRX cells (Fig. 3D).

DISCUSSION

Liver fibrosis represents the consequence of a continuous cycle of wound healing response to chronic hepatic injuries. Putative anti-fibrogenic drugs include bioactive agents that are able to reduce the activated HSC population by promoting cell apoptosis or the return of cells into the quiescence phenotype [Bataller and Brenner, 2005; Friedman, 2008].

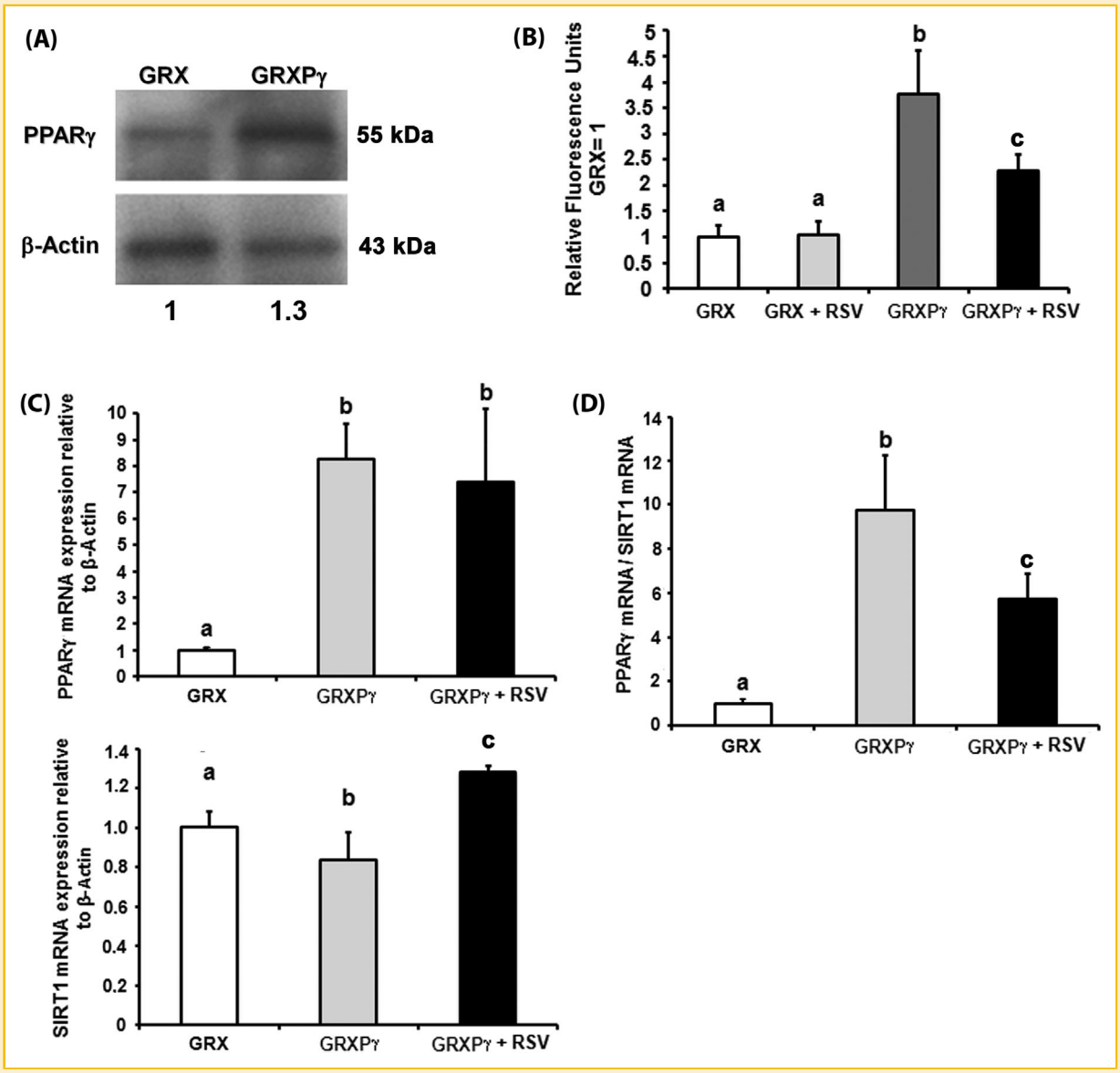

Fig. 3. Effects of RSV on super expressing PPARγ cells (GRXPγ). Immunoblotting analysis confirmed that GRXPγ presented an increase (30%) on the PPARγ protein content (A). GRXPγ cells naturally presented an increase on the intracellular lipids droplets content that was reduced by the half by RSV treatment (B). The RT-PCR evaluation of the PPARγ and SIRT1 mRNA expression unveiled that GRXPγ cells presented a decrease on the SIRT1 expression that was reverted to higher levels than untreated GRX (C). The PPARγ/SIRT1 ratio revealed that PPARγ mRNA expression was favoured over SIRT1 in RHO-treated cells. RSV treatment was able to reduce the PPARγ/SIRT1 ratio that remained higher than untreated GRX (D). Means without a common letter are statistically different ($n = 3$, $P \leq 0.05$).

GRX cell line represents the activated HSC phenotype and can be in vitro reverted to the quiescent phenotype, characterized by storing of cytoplasmic lipid droplets [Margis and Borojevic, 1989; Guaragna et al., 1992; Andrade et al., 2003]. PPAR proteins are pivotal for the regulation of lipid and glucose metabolism in numerous tissues [Kersten et al., 2000]. Lipogenesis in HSC is similar to adipogenesis in adipocytes, and PPARγ is known to regulate the transcriptional activation required in this process [Matsusue et al., 2004; Guimaraes et al., 2007]. Indeed, PPARγ exerts an important role in controlling the HSC quiescence state since cells activation and liver fibrosis development depend on a reduction of its expression. Furthermore, the in vitro or the in vivo treatment of activated HSC with PPARγ-ligands inhibits cell proliferation and the expression of both α-SMA type I collagen and monocyte chemotactic protein 1, a potent chemokine secreted by activated HSC that recruits and activates monocytes and T-lymphocytes [Miyahara et al., 2000; Eng and Friedman, 2001; Hazra et al., 2004].

The deacetylase SIRT1 plays an important role in a wide variety of cell processes, including stress resistance, metabolism and differentiation [Picard et al., 2004]. Unlike PPARγ, it has been already reported that the activation of SIRT1 results in a reduction of fat accumulation, an increase of free fatty acid release, and an inhibition of adipogenesis [Picard et al., 2004]. In mammals, SIRT1 regulates fat metabolism and hepatic glucose homeostasis through the modification of the PPARγ co-activator (PGC-1α) [Picard et al., 2004]. RSV can enhance SIRT1-dependent cellular processes by increasing its activity by as much as 8-fold and by decreasing the Km value for acetylated substrates to a much lesser extent than NAD [Howitz et al., 2003; Araki et al., 2004]. We have previously shown that RSV was able to trigger cell cycle arrest and apoptosis of the activated GRX cells in a pro-oxidative way. Interestingly, the RSV effects were dose-dependent. RSV concentrations up to 50 μM triggered cell resistance against its cytotoxic effects and only higher concentrations were able to effectively reduce the GRX cell population, which is an important way for liver fibrosis resolution [Souza et al., 2008; Martins et al., 2014a,b]. In the present study, we explored the effects of low doses of RSV (0.1 μM) on GRX quiescence through the action of PPARγ and SIRT1 on cell lipogenesis.

The protocol for GRX lipogenesis induction to effectively promote visual lipid droplet accumulation in the cell cytoplasm, predicts a minimum of 120 h treatment [Margis and Borojevic, 1989]. We found here that RSV was not able to induce lipogenesis in GRX while RHO was responsible for inducing the lipid droplets accumulation in these cells as previously shown by Borojevic and colleagues [Borojevic et al., 1991]. Interestingly, co-treated cells also presented an increase of cytoplasmic lipid droplets, but the [^{14}C] acetate incorporation into TG in this group was similar to the untreated or RSV-treated groups, a fact that may be related to a lipogenesis failure. We did not found a statistical difference when we individually analyzed protein content for PPARγ and SIRT1. However, when a ratio between these proteins content was established, the quantity of PPARγ protein in RHO- and co-treated cells was significantly higher than the quantity of SIRT 1 after 120 h of treatment.

It was already demonstrated that several enzymes of lipid metabolism are up-regulated in the early stages of GRX cell lipocyte induction [Vicente et al., 1997]. Thus, considering that PPARγ and SIRT1 may interfere on the enzymatic activity involved on the lipid metabolism, it was evaluated their mRNA expression after 12, 24, and 120 h of treatment. Interestingly, RHO treatment induced an increase of PPARγ mRNA expression from 12 h of GRX treatment whereas the RSV treatment induced an increase of SIRT1 mRNA only after 120 h. Thus, it is possible to state that the RHO induction of PPARγ transcription occurs faster than the RSV induction of SIRT1 transcription. Indeed, it seems to be of the upmost importance to observe that, after 120 h, the values for the ratio between mRNA expression of PPARγ and SIRT1 in co-treated cells remained higher than the observed in the untreated cells, but lower than the observed in RHO-treated cells. The RSV-mediated SIRT1 induction could effectively interfere on PPAR activity after 120 h of treatment, and this fact could explain why the co-treated cells showed an accumulation of cytoplasmic lipid droplets despite showing an incorporation of [^{14}C] acetate into TG similar to the untreated or RSV-treated cells.

To reinforce the role of the PPARγ/SIRT1 ratio on contributing to the lipogenesis of HSC, we established a permanent cell line that constitutively super expresses PPARγ (GRXPγ). Curiously, the simple fact of GRXPγ super express PPARγ induced the accumulation of lipid droplets in a spontaneous way, i.e., without any induction treatment, as a quiescent cell. RSV treatment was able to reduce this accumulation by the half. The mRNA of SIRT1 was slight decreased in untreated GRXPγ cells and was significantly increased in RSV-treated GRXPγ. These results suggest that stimulation of PPARγ mRNA expression could modulate SIRT1 mRNA expression and vice versa. Indeed, GRXPγ cells presented higher values for the PPARγ/SIRT1 ratio while RSV treatment induced a reduction in this parameter that anyway remained higher than that found in GRX cells.

In the present study, we found that 0.1 μM of RSV was not able to restore the HSC capacity of storing lipid droplets. These results are in accordance to those found by other authors who showed that RSV did not promote the differentiation of pre-adipocytes into adipocytes by not promoting adipogenesis [Rayalam et al., 2008]. In addition, our results raised the possibility that SIRT1 could play a role on modulating lipolysis in HSC and provided an in vitro evidence that the PPARγ/SIRT1 mRNA ratio could participate in the pathogenesis of liver fibrosis through regulating HSC quiescence or activation. Indeed, PPARγ seemed to be a potential key regulator in the activated HSC transition to the quiescent state. Thus, drugs that modulate its expression/activity could control the HSC phenotypic transformation. In this way, we understand that whenever the PPARγ mRNA expression is greater than SIRT1 mRNA expression the lipogenesis enabled (Fig. 4).

RSV is known to have a wide range of biological effects. We have previously showed that this phytoalexin reduced the population of activated HSC by triggering apoptosis. Importantly, this cellular response was largely depending on its concentration [Souza et al., 2008; Martins et al., 2014a,b]. Here we found that RSV can regulate the quiescence-like induction of HSC because the phytoalexin-mediated SIRT1 induction greatly interferes in the PPARγ-mediated lipogenesis. Further investigations on the effects of the RSV or SIRT1 in the molecular interactions that promote these aforementioned results are undoubtedly necessary to better understand the RSV contribution for the liver fibrosis resolution.

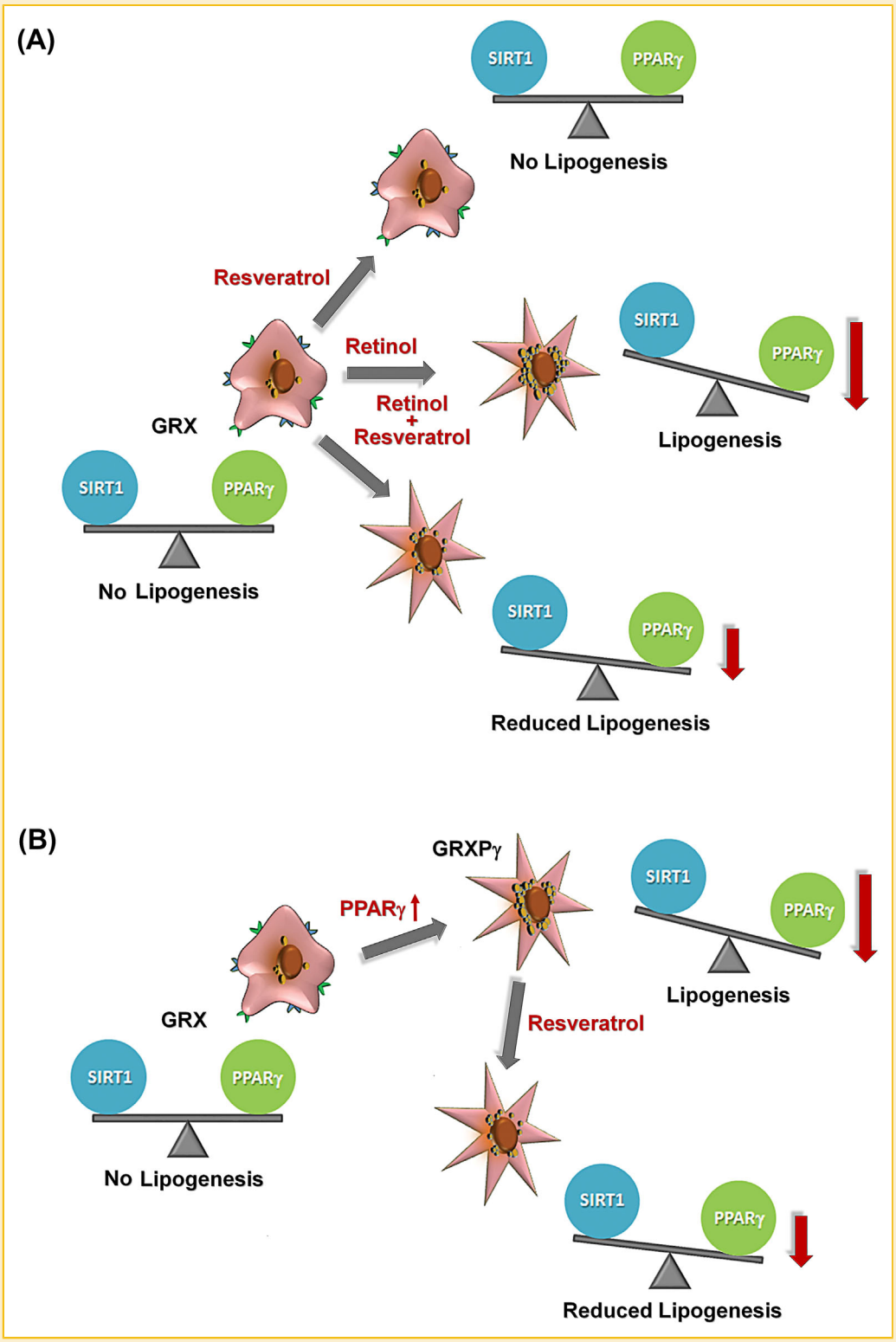

Fig. 4. Schematic illustration showing an overall view of the GRX and GRXPγ lipogenesis after 120 h of cell culture. For a detailed explanation of this figure, see text. RSV did not interfere on PPARγ/SIRT ratio and no lipogenesis was observed. RHO treatment induced the mRNA expression of PPARγ, which was broadly favoured over the mRNA expression of SIRT1. The RSV-mediated increase of the SIRT1 mRNA interfered in the RHO-mediated increase of the PPARγ mRNA after 120 h of treatment, thus reducing cell lipogenesis by promoting the decrease on the ratio between these molecules (A). The PPARγ super expression has led the GRX cells to lipogenesis. The RSV-mediated SIRT1 mRNA expression interfered in this process by reducing the PPARγ/SIRT1 ratio (B).

ACKNOWLEDGEMENTS

I.C.C. de Souza is the recipient of a fellowship from CNPq - Brazil. This work was also supported by CAPES, FAPERGS, and PROPESQ-UFRGS.

REFERENCES

Ahn J, Lee H, Jung CH, Jeon TI, Ha TY. 2013. MicroRNA-146b promotes adipogenesis by suppressing the SIRT1-FOXO1 cascade. Embo Mol Med 5:1602–1612.

Andrade CM, Trindade VM, Cardoso CC, Ziulkoski AL, Trugo LC, Guaragna RM, Borojevic R, Guma FC. 2003. Changes of sphingolipid species in the phenotype conversion from myofibroblasts to lipocytes in hepatic stellate cells. J Cell Biochem 88:533–544.

Araki T, Sasaki Y, Milbrandt J. 2004. Increased nuclear NAD biosynthesis and SIRT1 activation prevent axonal degeneration. Science 305:1010–1013.

Backesjo CM, Li Y, Lindgren U, Haldosen LA. 2009. Activation of SIRT1 decreases adipocyte formation during osteoblast differentiation of mesenchymal stem cells. Cells Tissues Organs 189:93–97.

Bataller R, Brenner DA. 2005. Liver fibrosis. J Clin Invest 115:209–218.

Bitencourt S, de Mesquita FC, Caberlon E, da Silva GV, Basso BS, Ferreira GA, de Oliveira JR. 2012. Capsaicin induces de-differentiation of activated hepatic stellate cell. Biochem Cell Biol 90:683–690.

Borojevic R, Monteiro AN, Vinhas SA, Domont GB, Mourao PA, Emonard H, Grimaldi G, Jr., Grimaud JA. 1985. Establishment of a continuous cell line from fibrotic schistosomal granulomas in mice livers. In Vitro Cell Dev Biol 21:382–390.

Borojevic R, Guaragna RM, Margis R, Dutra HS. 1990. In vitro induction of the fat-storing phenotype in a liver connective tissue cell line-GRX. In Vitro Cell Dev Biol 26:361–368.

Borojevic R, Guaragna RM, Margis R, Margis MP, Vicente CP, Silva LC. 1991. *In Vitro* Conversion of hepatic myofibroblast cell line GRX into lipocytes (Ito cells). Cells of the hepatic sinusoid 3:249–252.

Cheng Y, Ping J, Xu LM. 2007. Effects of curcumin on peroxisome proliferator-activated receptor gamma expression and nuclear translocation/redistribution in culture-activated rat hepatic stellate cells. Chin Med J (Engl) 120:794–801.

Desvergne B. 2008. PPARdelta/beta: The lobbyist switching macrophage allegiance in favor of metabolism. Cell Metab 7:467–469.

Eng FJ, Friedman SL. 2001. Transcriptional regulation in hepatic stellate cells. Semin Liver Dis 21:385–395.

Folch J, Lees M, Sloane Stanley. 1957. A simple method for the isolation and purification of total lipides from animal tissues. J Biol Chem 226:497–509.

Friedman SL. 2008. Mechanisms of hepatic fibrogenesis. Gastroenterology 134:1655–1669.

Guaragna RM, Trugo L, Borojevic R. 1992. Phospholipid modifications during conversion of hepatic myofibroblasts into lipocytes (Ito-cells). Biochim Biophys Acta 1128:237–243.

Guimaraes EL, Franceschi MF, Grivicich I, Dal-Pizzol F, Moreira JC, Guaragna RM, Borojevic R, Margis R, Guma FC. 2006. Relationship between oxidative stress levels and activation state on a hepatic stellate cell line. Liver Int 26:477–485.

Guimaraes EL, Franceschi MF, Andrade CM, Guaragna RM, Borojevic R, Margis R, Bernard EA, Guma FC. 2007. Hepatic stellate cell line modulates lipogenic transcription factors. Liver Int 27:1255–1264.

Hazra S, Xiong S, Wang J, Rippe RA, Krishna V, Chatterjee K, Tsukamoto H. 2004. Peroxisome proliferator-activated receptor gamma induces a phenotypic switch from activated to quiescent hepatic stellate cells. J Biol Chem 279:11392–11401.

Howitz KT, Bitterman KJ, Cohen HY, Lamming DW, Lavu S, Wood JG, Zipkin RE, Chung P, Kisielewski A, Zhang LL, Scherer B, Sinclair DA. 2003. Small molecule activators of sirtuins extend Saccharomyces cerevisiae lifespan. Nature 425:191–196.

Kersten S, Desvergne B, Wahli W. 2000. Roles of PPARs in health and disease. Nature 405:421–424.

Livak KJ, Schmittgen TD. 2001. Analysis of relative gene expression data using real-time quantitative PCR and the 2(-Delta Delta C(T)) Method. Methods 25:402–408.

Margis R, Borojevic R. 1989. Retinoid-mediated induction of the fat-storing phenotype in a liver connective tissue cell line (GRX). Biochim Biophys Acta 1011:1–5.

Martins LA, Coelho BP, Behr G, Pettenuzzo LF, Souza IC, Moreira JC, Borojevic R, Gottfried C, Guma FC. 2014a. Resveratrol induces pro-oxidant effects and time-dependent resistance to cytotoxicity in activated hepatic stellate cells. Cell Biochem Biophys 68:247–257.

Martins LA, Vieira M, Ilha M, de Vasconcelos M, Biehl H, Lima D, Schein V, Barbé-Tuana F, Borojevic R, Guma F. 2014b. The Interplay Between Apoptosis, Mitophagy and Mitochondrial Biogenesis Induced by Resveratrol Can Determine Activated Hepatic Stellate Cells Death or Survival. Cell Biochem Biophys 1–16.

Martucci RB, Ziulkoski AL, Fortuna VA, Guaragna RM, Guma FC, Trugo LC, Borojevic R. 2004. Beta-carotene storage, conversion to retinoic acid, and induction of the lipocyte phenotype in hepatic stellate cells. J Cell Biochem 92:414–423.

Matsusue K, Gavrilova O, Lambert G, Brewer HB, Ward JM, Inoue Y, LeRoith D, Gonzalez FJ. 2004. Hepatic CCAAT/enhancer binding protein alpha mediates induction of lipogenesis and regulation of glucose homeostasis in leptin-deficient mice. Mol Endocrinol 18:2751–2764.

Miyahara T, Schrum L, Rippe R, Xiong S, Yee HF, Jr., Motomura K, Anania FA, Willson TM, Tsukamoto H. 2000. Peroxisome proliferator-activated receptors and hepatic stellate cell activation. J Biol Chem 275: 35715–35722.

Peterson GL. 1979. Review of the Folin phenol protein quantitation method of Lowry, Rosebrough Farr and Randall. Anal Biochem 100:201–220.

Picard F, Kurtev M, Chung N, Topark-Ngarm A, Senawong T, Machado De Oliveira R, Leid M, McBurney MW, Guarente L. 2004. Sirt1 promotes fat mobilization in white adipocytes by repressing PPAR-gamma. Nature 429:771–776.

Rayalam S, Della-Fera MA, Baile CA. 2008. Phytochemicals and regulation of the adipocyte life cycle. J Nutr Biochem 19:717–726.

Song C, Kokontis JM, Hiipakka RA, Liao S. 1994. Ubiquitous receptor: a receptor that modulates gene activation by retinoic acid and thyroid hormone receptors. Proc Natl Acad Sci U S A 91:10809–10813.

Souza IC, Martins LA, Coelho BP, Grivicich I, Guaragna RM, Gottfried C, Borojevic R, Guma FC. 2008. Resveratrol inhibits cell growth by inducing cell cycle arrest in activated hepatic stellate cells. Mol Cell Biochem 315: 1–7.

Teboul M, Enmark E, Li Q, Wikstrom AC, Pelto-Huikko M, Gustafsson JA. 1995. OR-1, a member of the nuclear receptor superfamily that interacts with the 9-cis-retinoic acid receptor. Proc Natl Acad Sci U S A 92:2096–2100.

Teodoro AJ, Perrone D, Martucci RB, Borojevic R. 2009. Lycopene isomerisation and storage in an in vitro model of murine hepatic stellate cells. Eur J Nutr 48:261–268.

Vicente CP, Guaragna RM, Borojevic R. 1997. Lipid metabolism during in vitro induction of the lipocyte phenotype in hepatic stellate cells. Mol Cell Biochem 168:31–39.